

# Thermodynamics and molecular insight in guest–host complexes of fluoroquinolones with $\beta$ -cyclodextrin derivatives, as revealed by ATR-FTIR spectroscopy and molecular modeling experiments

Irina M. Le-Deygen<sup>1</sup>  · Anna A. Skuredina<sup>1</sup> · Igor V. Uporov<sup>1</sup> · Elena V. Kudryashova<sup>1</sup>

Received: 26 April 2017 / Revised: 11 August 2017 / Accepted: 17 August 2017  
© Springer-Verlag GmbH Germany 2017

**Abstract**  $\beta$ -Cyclodextrin (CD) is a perspective class of excipients used in pharmaceutical formulations to enhance solubility, bioavailability, and pharmacokinetics of various poorly soluble drugs, forming a non-covalent guest–host complex. However, the development of such formulations is usually a very laborious and time-consuming process due to lack of appropriate analytical tools to directly track and study the detailed molecular mechanism of such complex formation. Here, using guest–host complexes of fluoroquinolones (FQ) with CDs, as an example, we demonstrate the utility of ATR-FTIR to determine the thermodynamic stability, as well as structural features associated with complex formation, including involvement of certain functional groups. Furthermore, varying the CD's side groups, we were able to tailor the CD's geometry and binding surface to make FQ–CD interactions strong enough to potentially affect its pharmacokinetics and justify development of a new sustained-release drug formulation (dissociation constant decreased from  $5 \cdot 10^{-3}$  M to  $10^{-5}$  M). 3D molecular modeling with energy optimization supports the findings and conclusions made on the basis of ATR-FTIR data analysis and explains the observed difference in dissociation constants.

**Keywords** Fluoroquinolones ·  $\beta$ -Cyclodextrin · Guest–host complexes · ATR-FTIR spectroscopy

**Electronic supplementary material** The online version of this article (<https://doi.org/10.1007/s00216-017-0590-5>) contains supplementary material, which is available to authorized users.

✉ Irina M. Le-Deygen  
i.m.deygen@gmail.com

<sup>1</sup> Department of Chemistry, Lomonosov Moscow State University, Leninskie gory, 13, 119991 Moscow, Russia

## Abbreviations

CD	Cyclodextrin
FQ	Fluoroquinolones
HPCD	2-Hydroxypropyl- $\beta$ -cyclodextrin
LF	Levofloxacin
MCD	Methyl- $\beta$ -cyclodextrin
MF	Moxifloxacin
SBECD	Sulphobutyl ether $\beta$ -cyclodextrin
TB	Tuberculosis

## Introduction

Treatment of newly diagnosed intracellular infections of tuberculosis (TB) usually involves a combination of 4–5 front-line antibiotics, administered daily for 6–12 months. Such treatment is often associated with adverse side effects and poor patient compliance [1]. Over the last decades the occurrence of multi-resistant and pan-resistant *Mycobacterium tuberculosis* strains has been documented with ever increasing frequency. Therapy of multi-resistant TB with second-line combination drugs (levofloxacin, ciprofloxacin, clofazamine, ethionamide, kanamycin, etc.) lasts much longer (24–48 months) and is associated with even more frequent and adverse side effects. For fluoroquinolones (FQ), which are widely used both as front-line and second-line anti-TB therapy, the adverse effects involve phototoxicity, seizures, hemodynamic disorders, and increased risks of thrombosis. Half-life and bioavailability of many FQ are also far from being optimal. Safety and pharmacokinetic profile of some pharmaceuticals, including anti-TB drugs, can be improved by developing controlled drug release formulations [2]. Guest–host complex formation with cyclodextrins (CDs), a family of macrocyclic oligosaccharides linked by  $\alpha$ -1,4 glycosidic bonds, is one of the perspective approaches in this area.

Truncated cone-shaped  $\beta$ -CD molecule possesses a hollow cavity of 0.79 nm in depth. The top and bottom diameters are increased with the number of glucose units composing CDs [3]. The hollow cavity of CDs is hydrophobic, thus rendering guest-host binding capacity for a variety of compounds ranging from small molecules to proteins. CDs are able to form water-soluble inclusion complexes with many poorly soluble lipophilic drugs. Thus, CDs are used to enhance the aqueous solubility of drugs and to improve drug bioavailability after, for example, oral administration. Through CD complexation, poorly soluble drugs can be formulated as aqueous parenteral solutions, nasal sprays, and eye drop solutions. These oligosaccharides are being recognized as non-toxic and pharmacologically inactive excipients for medicinal substances. CDs are known for their multiple possibilities for derivatization, enabling creation of libraries of functionalized compounds. Moreover, some derivatives, such as 2-hydroxypropyl, methyl, and sulphobutyl ether CDs, possess improved toxicological profiles in comparison to the parent CDs. Due to their high tolerance in the human body, the substituted CDs open new doors in the development of injectable formulations with improved efficiency.

Currently, there are over 35 approved drugs based on CD complexes, and still for many pharmaceuticals, including FQ, the potential pharmacokinetic and safety improvement from complex formation with CDs may be largely underexplored. One of the reasons for that is the lack of appropriate analytical tools to directly track and study the detailed molecular mechanism of complex formation depending on the FQ structure and side group in CDs. Here, we demonstrate the use of ATR-FTIR in aqueous solution to investigate the thermodynamic stability of the complexes, as well as their structural features, including determination of the binding sites of FQ with CDs and involvement of certain functional groups in the complex formation.

This kind of information about complex formation mechanism in aqueous solution cannot be obtained by any other single method applied previously for such studies, including UV and fluorescence spectroscopy, NMR spectroscopy and differential scanning calorimetry, SERS spectroscopy, and liquid chromatography [4–8]. In this study, we have investigated the molecular insight in complex formation of FQ used in anti-TB therapy, levofloxacin (LF), and moxifloxacin (MF), with  $\beta$ -cyclodextrin derivatives, including 2-hydroxypropyl- $\beta$ -cyclodextrin (HPCD), methyl- $\beta$ -cyclodextrin (MCD), and sulphobutyl ether  $\beta$ -cyclodextrin (SBECD). In order to decipher the interaction mechanism in greater detail, 3D molecular modeling with energy optimization was applied. We have shown that depending on the nature of substituent the physico-chemical parameters of complex formation can differ by an order of magnitude, which is explained by different molecular geometry and consequently, different mechanism of the complex stabilization.

## Experimental

**Chemicals** Methyl- $\beta$ -cyclodextrin, sulphobutyl ether  $\beta$ -cyclodextrin, and 2-hydroxypropyl- $\beta$ -cyclodextrin were obtained from Sigma (USA), levofloxacin from Zhejiang Kangyu Pharm Co Ltd. (China), and moxifloxacin from Sansh Biotech Pvt. Ltd. (India).

**Preparation of the complexes of fluoroquinolones with 2-hydroxypropyl- $\beta$ -cyclodextrin, methyl- $\beta$ -cyclodextrin, and sulphobutyl ether  $\beta$ -cyclodextrin** A solution of corresponding FQ (2–4 mg/mL, in 15 mM potassium-phosphate buffer, pH 7.0 or in hydrochloric acid solution, pH 2–4) was mixed with a solution of  $\beta$ -CD in the same buffer solution (pH 2–7). The molar excess of  $\beta$ -CD:FQ was varied from 0.25 to 10.0. The complexes were incubated under stirring at 37 °C for 60 min.

**ATR-FTIR** ATR-FTIR spectra were recorded using a Bruker Tensor 27 spectrometer equipped with a liquid nitrogen cooled MCT (mercury cadmium telluride) detector. Samples were placed in a thermostated cell BioATR-II with ZnSe ATR element (Bruker, Germany). The ATR-FTIR spectrometer was purged with a constant flow of dry air. ATR-FTIR spectra were acquired from 900 to 3000  $\text{cm}^{-1}$  with 1  $\text{cm}^{-1}$  spectral resolution. For each spectrum, 100 scans were accumulated at 20 kHz scanning speed and averaged. All spectra were registered in aqueous buffer solution: in 15 mM potassium-phosphate buffer, pH 7.0 or in hydrochloric acid solution, pH 2–4, at 22 °C, concentration of FQ was 1–4 mg/mL. To study spectral characteristics of FQ in the complexes FQ-CD, CD solution in the corresponding concentration was used as a blank, and vice versa, to study spectral characteristics of CDs the blank solution was the solution of FQ at corresponding concentration. Spectra of CDs are presented on Fig. S1 in the Electronic Supplementary Material (ESM). Spectral data were processed using the Bruker software system Opus 7.5 (Bruker, Germany), which includes linear blank subtraction, straight-line baseline correction, and atmosphere compensation [9, 10]. If necessary, seven- or nine-point Savitsky-Golay smoothing was used to remove white noise. Peaks were identified by standard Bruker picking-peak procedure.

**UV-spectroscopy** UV-spectroscopy was performed with Amersham Biosciences Ultraspec 2100 pro as it was described previously [11, 12]. One milliliter aliquots in 15 mM potassium-phosphate buffer, pH 7.0 or in hydrochloric acid solution (pH 2–4) was transferred into quartz cells 108-QS Hellma Analytics, UV-spectra were recorded 210–380 nm,  $T$  22 °C.

**Evaluation of  $K_{\text{dis}}$  values of the complexes** Evaluation of  $K_{\text{dis}}$  values of the complexes was conducted by UV-spectroscopy according to standard procedure described

elsewhere [4, 13]. Data analysis was carried using Benesi-Hildebrand Eq. (1).

$$\frac{1}{A-A_0} = \frac{K_{dis}}{(A_\infty-A_0) \times [CD]} + \frac{1}{A_\infty-A_0} \quad (1)$$

where  $A_0$  is the absorbance of MF,  $A$  is the absorbance of complex,  $A_\infty$  is the absorbance when all MF molecules are complexed by CD.

**ATR-FTIR spectroscopy evaluation of  $K_{dis}$  values of the complexes** To determine  $K_{dis}$  values of the complexes, the analysis of ATR-FTIR data was performed in Scatchard coordinates [9]. The equilibrium in the system containing FQ and CD can be described by the following scheme:



This scheme corresponds to the following equation for dissociation constant (2):

$$K_{dis} = \frac{[FQ]_f \times [CD]_f}{[FQ-CD]} \quad (2)$$

The material balance equations are as follows:

$$\begin{aligned} [FQ]_0 &= [FQ]_f + [FQ-CD], \\ [CD]_0 &= [CD]_f + [FQ-CD], \\ [FQ-CD] &= [CD]_b, \end{aligned}$$

where  $[CD]_0$ ,  $[CD]_f$ , and  $[CD]_b$  are the initial concentration of CD, concentration of “free,” and bound with FQ copolymer correspondingly;  $[FQ]_0$ ,  $[FQ]_f$ , and  $[FQ-CD]$  are the initial concentration of FQ, concentration of “free,” and bound with copolymer FQ correspondingly.

Scatchard transformation of  $K_{dis}$  equation leads to follow (3):

$$\frac{1}{K_{dis}} = \frac{[CD]_b}{[CD]_f \times (FQ_f - CD_b)} \quad (3)$$

or

$$\frac{[CD]_b}{[CD]_f} = \frac{1}{K_{dis}} \times [FQ]_0 - \frac{1}{K_{dis}} \times [CD]_b \quad (4)$$

The values of  $[CD]_b$  and  $[CD]_f$ , both in molar concentration, were plotted in Scatchard coordinates:  $[CD]_b/[CD]_f$  versus  $[CD]_b$  (according to Eq. (4)), and the dissociation constant

$K_{dis}$  was calculated by approximation of data by line. To control obtained values of  $K_{dis}$ , data was processed in Klotz coordinates (5):

$$\frac{1}{[FQ-CD]} = \frac{1}{K_{dis} \times [FQ]_0} \times \frac{1}{[CD]} + \frac{1}{[FQ]_0} \quad (5)$$

**Freeze-dry experiments** An aliquot of 500 mg of moxifloxacin was dissolved in HCl solution (pH 4) and mixed with CD solution in equimolar proportion. The mixture was stirred for 1 h at 30 °C followed by freezing at -70 °C for 24 h and further lyophilization for 24 h at -60 °C using a freeze-dryer (Thermo Scientific, USA).

**Scanning electron microscopy** Scanning electron microscopy (SEM) was performed by SEM Carl Zeiss LEO 1450 (Germany) as described before [12]. The tested samples were placed on a conductive (carbon) adhesive tape, onto which a thin film of gold (~0.05–0.1 μm) was applied next using the plasma spray technique to ensure the required electrical conductivity of the surface. Analysis of the sizes of micronized particles was performed with the help of the IP3 software.

**Molecular modeling** The structures of the molecules of fluoroquinolones and β-cyclodextrins were built in the software ChemBio3D (“CambridgeSoft”), which is part of the Perkin Elmer company. These structures were optimized by MOPAC2016 program using PM6 quantum chemistry semi empirical method. Optimized structures were converted to mol2 format using the OpenBabel 2.4.0 program followed by CHARMM27 topology and coordinates files generation by the SwissParam web service.

To examine the structural and dynamic characteristics of the complex, the molecular dynamics method was applied. The initial structures of the complexes and its components were placed in the center of the solvation sphere filled with the water molecules. The radius of the sphere was chosen in accordance with covering the studied system with a layer of water molecules not less than 20 Å. In the process of dynamics, the water molecule crossed the boundary of the solvation sphere, and then the force appeared to return it back into the sphere, allowing maintaining the constant number of water molecules in solvation sphere in the modeling process. To preserve the central position of the complex in the solvation sphere one of the atom’s position was fixed. Visual analysis of the trajectories showed that in the process of modeling the system was covered with a thick enough layer of water. After solvation and neutralization of the charge of the system (if required) the energy minimization (1000 steps) were conducted which followed by molecular dynamics at constant temperature (300 K) for 20 ns. The coordinates of the atoms remained after 2 ps for further analysis. Building the initial

structures of the complexes (manual docking of a molecule of FQ into the cavity of CD), preparation of spatial structures of molecules for molecular dynamics, solvation and neutralization of the charge of the system, the energy minimization, molecular dynamics, and visual analysis of the trajectories were performed using the software package VMD/NAMD developed by the theoretical and computational Biophysics in Baklanovka Institute University of Illinois at Urbana-Champaign.

Generalized Born implicit solvent (GBIS) method implemented in NAMD program was employed to model solvent around FQ, CD molecules, and their complex. For each saved frame of molecular dynamics trajectories, the potential energy difference between two particular molecules and their complex was calculated and averaged for all frames to be considered as mean energy complex formation energy which characterizes the affinity of molecules to each other.

*X-Ray analysis* was conducted with diffractometer D2 PHASER (Bruker, Germany) in following conditions: goniometry – vertical  $\theta / \theta$ , radius 141.5 mm, tube 2.2 kV with copper anode, and long thin linear focus ( $0.4 \times 12$  mm), generator 30 kV 10 mA, primary optics 0.4 mm with fixed gap, standard sample carrier with rotation, secondary optics—Ni-filter, the position-sensitive semiconductor detector LynxEye— $4^\circ$ . Powders were placed in a Plexiglas cell without adding any components and pressing and without further treatment to the flat and level surface. All radiographs were taken in increments of about 0.02 in the range of 4–50°. 2 rotation with 15 vol./min and holding at 0.5 s. Analysis of components of the system was carried out using the EVA program on the basis of PDF-4 Organic.

## Results and discussion

### ATR-FTIR spectra of fluoroquinolones: impact of pH

The ATR-FTIR spectra of unbound FQ, moxifloxacin (MF), and levofloxacin (LF), were studied at different pH for the reference and peak assignment. In spectra of LF and MF (Fig. 1), the main characteristic bands are 1720–1700 and 1630–1610  $\text{cm}^{-1}$ , corresponding to carboxyl and carbonyl group of quinolone fragment; bands at 1500–1430  $\text{cm}^{-1}$  assigned to oscillation of C–C bond in aromatic structure of quinolone; the band at 1050–1020  $\text{cm}^{-1}$  assigned to oscillation of C–F bond; band at 979  $\text{cm}^{-1}$  corresponding to C–N bond in piperazol cycle in LF [14–17].

Increase of pH from 2 to 4 and subsequently to pH 7 leads to noticeable changes in the ATR-FTIR spectrum of LF (Fig. 1a) due to the presence of two pH-sensitive ionogenic groups in the molecule: carboxyl group, conjugated with the aromatic structure of the quinolone with  $pK_a$  of 4.5, and piperazol N–H group, with  $pK_a$  of 8.0 [14, 15]. The most pronounced changes

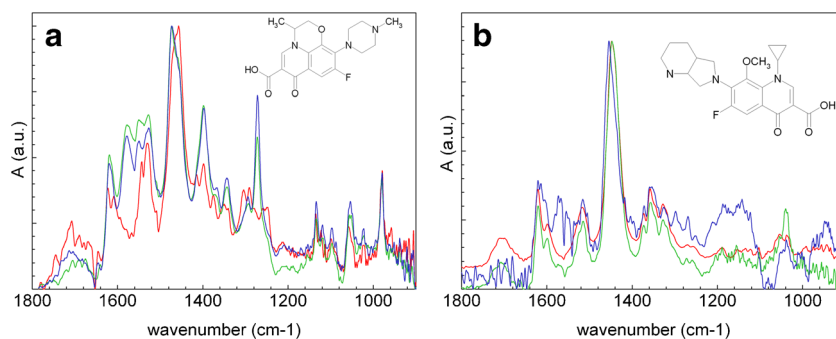
in the band fine structures as well as in their intensities are observed for the aromatic moiety of quinolone at 1500–1430  $\text{cm}^{-1}$ : high-frequency shift and intensity increase is observed due to effect of carboxyl group deprotonation on the stretching vibrations of C–C bonds in aromatic ring. Band of deprotonated carboxyl group (at 1580  $\text{cm}^{-1}$ ), absent at pH 2, becomes noticeable at pH 4 and 7; additional mode, corresponding to C–O bond in carboxylic group [17] can be observed at 1283–1270  $\text{cm}^{-1}$  at pH 4 and 7 (Fig. 1a). Bands in the region of 1050–1020  $\text{cm}^{-1}$ , assigned to the vibrations of C–F bond, and the band at 979  $\text{cm}^{-1}$  corresponding to piperazol structure, are less sensitive to pH in the interval from 2 to 7, since these groups do not change their ionic state in this pH range. Similar spectral changes with pH were observed for MF (Fig. 1b).

### Complex formation of levofloxacin with 2-hydroxypropyl- $\beta$ -cyclodextrin at pH 2

The binding sites and involvement of functional groups of LF in complex formation with HPCD was studied in the condition when carboxylic group in LF is neutral, while the amino group in piperazol is protonated. According to the literature, uncharged fragment of FQs would more likely be able to bind in the hydrophobic inner cavity of CD [18, 19], as it was shown for a number of organic molecules interacting with  $\beta$ -CD. Figure 2a shows ATR-FTIR spectra of LF in the complex with HPCD (1:1) as compared to unbound LF at pH 2. The complex formation leads to decrease in the intensity of the following adsorption bands of LF: carbonyl and carboxyl groups (1710–1600  $\text{cm}^{-1}$ ) as well as aromatic cycle bands (1500–1430  $\text{cm}^{-1}$ ) of quinolone. The band of piperazol cycle (at 976  $\text{cm}^{-1}$ ) does not undergo any changes upon the complex formation, thus confirming our assumption that only uncharged carbonyl and carboxyl groups as well as the hydrophobic aromatic quinolone moiety can dip into the inner cavity of HPCD upon interaction (Fig. 2a insertion).

In order to determine the LF – HPCD dissociation constant ( $K_{\text{dis}}$ ) at pH 2, LF spectra at different LF/HPCD molar ratios was investigated. Figure 2b presents ATR-FTIR spectra of LF–HPCD complexes in the region of aromatic moiety (1500–1430  $\text{cm}^{-1}$ ) where the most pronounced changes in spectra of LF upon complexation are observed. Deconvolution of this spectral region in the absence of HPCD reveals three main components: 1475, 1455, and 1463  $\text{cm}^{-1}$  (Fig. 3a). Addition of HPCD with increasing molar ratio up to 10:1 leads to gradual decrease of the relative integral intensity at 1463  $\text{cm}^{-1}$ ; in the excess of HPCD, this spectral component is absent (Fig. 3b). This phenomenon can be explained considering that component at 1463  $\text{cm}^{-1}$  corresponds to aromatic fragment in hydrophilic microenvironment. The contribution of this component decreases upon entrapping of FQ into CD cavity with more hydrophobic media. The analysis of relative integral intensities yields the binding

**Fig. 1** ATR-FTIR spectra of **a** levofloxacin and **b** moxifloxacin in buffer solutions with variable pH: 2 (red plot), 4 (green plot), 7 (blue plot). Fluoroquinolones concentration was 1 mg/mL, 22 °C. Spectra are min–max normalized for better representation



isotherm for LF–HPCD system (Fig. 3b insertion). Linearization of this isotherm in Scatchard coordinates gives the complex composition of 1:1 and  $K_{dis}$  value of  $9 \times 10^{-4}$  M, which is in a good agreement with  $K_{dis}$  obtained by other techniques for inclusion complexes of CDs with FQ including levofloxacin and moxifloxacin ( $1 \times 10^{-5}$ – $4 \times 10^{-3}$  M) [19–22].

### Complex formation of LF and MF with 2-hydroxypropyl- $\beta$ -cyclodextrin (HPCD) at pH 4 and 7

Similarly to pH 2, complex formation of LF–HPCD and MF–HPCD at pH 4 results in significant changes in the LF and MF IR spectra in region of carbonyl and carboxyl groups ( $1720$ – $1600$   $\text{cm}^{-1}$ ) and in C–C bonds of the aromatic structure of quinolone ( $1500$ – $1430$   $\text{cm}^{-1}$ ). Spectra of MF–HPCD complexes depending on the MF–HPCD molar ratio formed at pH 4 are presented in Fig. 4a as an example. Analysis of the binding isotherm of MF–HPCD obtained on the base of the decrease in the peak intensities at  $1500$ – $1430$   $\text{cm}^{-1}$  (Fig. 4b) yields a  $K_{dis}$  value of  $3.3 \times 10^{-3}$  M. For LF–HPCD complex, the  $K_{dis}$  value was evaluated as  $1 \times 10^{-3}$  M (Table 1). These  $K_{dis}$  values are of the same order of magnitude as  $K_{dis}$  found for complex of LF–HPCD at pH 2 and in agreement with values obtained in previous studies [21, 22].

At pH 7 the FQ carboxylic groups are charged (deprotonated) and complex formation with CDs is accompanied by much weaker spectral changes than in acidic media, suggesting higher dissociation constant. This is in agreement

with the data obtained elsewhere, where a negative or positive charge of guest molecules results in a 2- to 10-fold drop in the binding constant of CD–substrate complexes compared to the neutral forms of the same ligands [19]. Thus, acidic media favors the complex formation of FQs with CDs. However the potential practical use of the complexes as drug delivery systems requires their stability at physiological pH. So, the complex stability after “pH-stress” (transition from pH 4.0 to pH 7.0) was studied. The spectral analysis of LF–HPCD and MF–HPCD complexes formed at pH 4 and transferred to pH 7.0, suggests that the complex does not show any noticeable dissociation for at least 2 h due to kinetic barrier. So, formed at low pH, the complex is stable at pH 7, potentially enabling intravenous application with sustained release.

### Tailoring CD structure site for stronger binding with FQ

To explore the possibility of targeted, ATR-FTIR-assisted design of FQ–CD complex, we have studied substituted CD molecules. CD’s core structure enables side group derivatization with substituents of different nature, generating a library of compounds with different geometry and properties of the binding site. Besides HPCD (carrying polar group), we have studied FQ complex formation parameters with MCD (modified with hydrophobic group) and SBCD (modified with charged sulpho group) (ESM Fig. S2). The binding constant achieved for HPCD–MF complex was  $10^{-3}$  M, while for the complex to enable sustained release of the target drug in vivo, the binding constant has to be in the order of  $10^{-5}$  M [20].

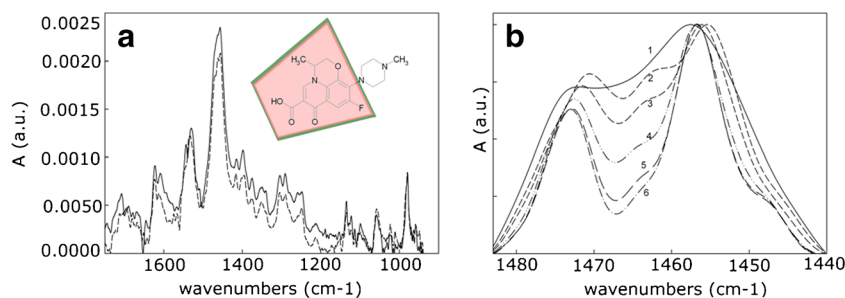


**Fig. 2** **a** ATR-FTIR spectra of LF (line) and complex LF–HPCD 1:1 (dashed line), pH 2, LF concentration was 1 mg/mL. Insertion: Proposed structure of LF–HPCD complex. **b** Spectral region of aromatic C–C bond adsorption: LF (1), LF–HPCD with molar ratios of 1:0.25 (2),

1: 0.5 (3), 1:1(4), 1:5(5), and 1:10 (6). Spectrum of CD has been subtracted as a blank. Spectra are min–max normalized on Fig. 2b for better representation

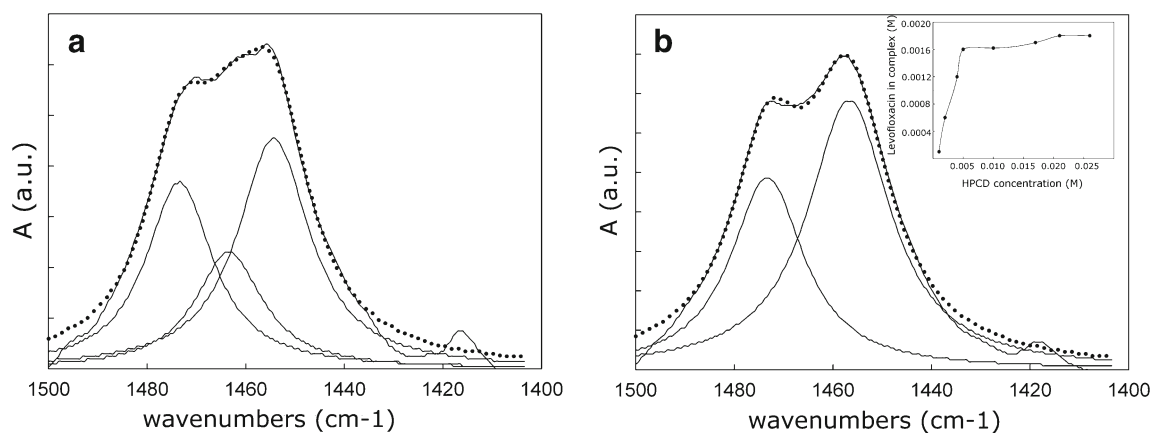


**Fig. 3** Deconvolution of the ATR-FTIR spectra region corresponding to adsorption of C–C band in aromatic structure of LF (a) and LF–HPCD 1:10 complex (b). Insertion: Dependence of concentration of LF involved

in the complex on molar excess of HPCD. Concentration of LF 1 mg/ml, pH 2, 22 °C

Interaction with SBECD and MCD at pH 4 led to the similar changes in MF spectra as it was observed for the complexes with HPCD: intensity of main bands in the regions of carbonyl group (1650–1600  $\text{cm}^{-1}$ ) and C–C bonds of the aromatic structure of quinolone (1480–1440  $\text{cm}^{-1}$ ) decreases gradually with increase in CD concentration (Fig. 4c, d). Noteworthy that for MF, absorption band at 1580  $\text{cm}^{-1}$ , assigned to deprotonated carboxylic group, disappears upon the complex formation with HPCD, SBECD, and MCD suggesting the involvement of carboxylic group in the interaction with CD. Since carboxylate ion is energetically unfavorable in the hydrophobic environment of CD cavity, in contrast to unbound MF, COOH group of MF in MF–CDs complexes is protonated. The binding isotherms for MF–SBECD and MF–MCD based on the decrease in the overall band intensity at 1500–1400  $\text{cm}^{-1}$  with increase in the CDs concentration are presented in Fig. 4d. Linearization of these isotherms in Scatchard coordinated (ESM Fig. S3) and in Klotz coordinates (ESM Fig. S4) yields to  $K_{\text{dis}}$  values of  $5 \times 10^{-5}$  M for MF–MCD and  $1 \times 10^{-4}$  M for MF–SBECD (Table 1).

In the case of complex formation of MF with MCD in addition to abovementioned changes in the bands intensities, the pronounced changes in fine structure of the band of quinolone core at 1500–1430  $\text{cm}^{-1}$  are observed. Deconvolution analysis of this band provides further detail on the MF interaction with MCD. For free MF three components can be found at: 1440, 1452, and 1463  $\text{cm}^{-1}$ ; the complex formation leads to decrease in the relative contribution of the components at 1463 and 1452  $\text{cm}^{-1}$  (Fig. 5) while the relative integral intensity of the low-frequency component (at 1440  $\text{cm}^{-1}$ ) increases. Similarly to the picture observed for the complex of LF with HPCD discussed above, this phenomenon can be explained by entrapping of aromatic fragment of MF from aqueous microenvironment into MCD hydrophobic cavity.

Deconvolution analysis of the band 1500–1430  $\text{cm}^{-1}$  for MF–MCD yields the  $K_{\text{dis}}$  value of  $8.6 \times 10^{-5}$  M, which is in the good agreement with  $K_{\text{dis}}$  found by the intensities analysis (Table 1). So, the changes in intensity and in fine structure of the band of quinolone core at 1500–1430  $\text{cm}^{-1}$  are likely to reflect the same complex formation-associated process. The

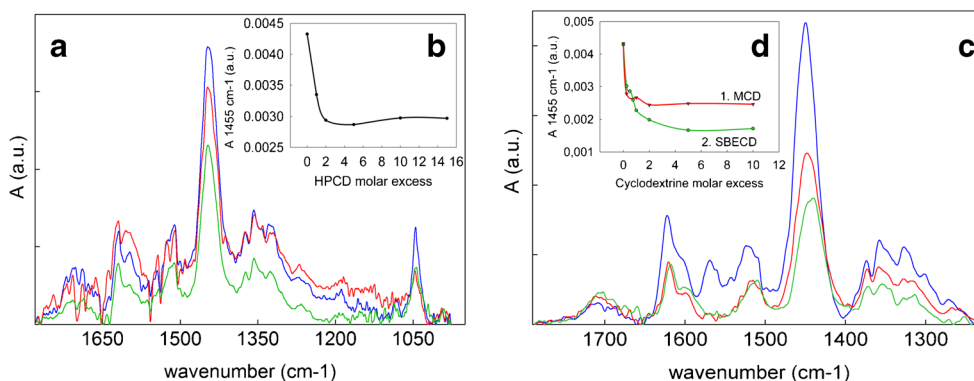


**Fig. 4** a ATR-FTIR spectra of moxifloxacin (blue) and complexes moxifloxacin–HPCD 1:1 (red) and 1:10 (green). b Dependence of concentration of moxifloxacin involved in the complex on molar excess of HPCD. c ATR-FTIR spectra of moxifloxacin (blue) and complexes moxifloxacin–MCD 1:10 (red) and moxifloxacin–SBECD 1:10 (green).

d Dependence of concentration of MF involved in the complex on molar excess of MCD and SBECD. Concentration of moxifloxacin 1 mg/ml, pH 4, 22 °C. Spectrum of corresponding CD has been subtracted as a blank

**Table 1** Values of dissociation constants ( $K_{dis}$ ) of the MF and LF complexes with  $\beta$ -cyclodextrins evaluated by ATR-FTIR spectroscopy and UV-spectroscopy. Standard deviation (SD,  $n = 3$ )

FQ	HPCD, M		SBECD, M		MCD, M	
MF	$3.3 (\pm 0.3) \times 10^{-3}$ (ATR-FTIR)	$2.6 (\pm 0.8) \times 10^{-3}$ (UV)	$1.0 (\pm 0.3) \times 10^{-4}$ (ATR-FTIR)	$3.3 (\pm 1.1) \times 10^{-4}$ (UV)	$5.0 (\pm 0.3) \times 10^{-5}$ (ATR-FTIR)	$4.0 (\pm 0.9) \times 10^{-5}$ (UV)
LF	$1.0 (\pm 0.3) \times 10^{-3}$ (ATR-FTIR)		$5.0 (\pm 0.3) \times 10^{-5}$ (ATR-FTIR)		$1.0 (\pm 0.3) \times 10^{-4}$ (ATR-FTIR)	

agreement of the  $K_{dis}$  value obtained by these two approaches confirms the validity of the results and provides complementary information on the complex properties.

### Complex formation of LF with SBECD and MCD

Similarly to MF, the spectral changes observed upon the complex formation of LF with SBECD and MCD are more pronounced compared to the complexes with HPCD (Fig. 6), suggesting tighter binding of LF in the SBECD and MCD cavity compared to HPCD. The corresponding binding isotherms based on the decrease in the overall band intensity of LF at  $1500\text{--}1400\text{ cm}^{-1}$  with increase in the CDs concentration are presented in Fig. 6 (insert).  $K_{dis}$  for LF-SBECD and LF-MCD complexes were evaluated as  $5 \times 10^{-5}$  and  $1 \times 10^{-4}$  versus  $1 \times 10^{-3}$  M for complex with HPCD (Table 1). So, for LF, similarly to MF, use of SBECD and MCD resulted in the formation of 5–10 times more stable complex compared to that for HPCD (Table 1). This can be explained by the presence of additional complex-stabilizing factors: hydrophobic interaction of LF molecule with methyl group in case of the complex with MCD and interaction of cationic sites (piperazol group) in LF with sulphobutyl group of SBECD. In the case of the complex with SBECD the interaction between cationic sites (piperazol group) in LF with sulphobutyl group of SBECD is observed, as evidenced by decrease in the intensity of the absorption band of piperazol group in LF at  $975\text{ cm}^{-1}$  in LF spectrum (Fig. 6). This effect was much less pronounced in the case of LF complex with HPCD (Fig. 2a).

As a validation control, dissociation constants for MF-CDs complexes were also measured with a well-characterized

method based on the change in intensity of the absorption band at 290 nm in UV-spectrum of MF upon the complex formation with CDs [4].  $K_{dis}$  were evaluated according to the Benesi-Hildebrand equation [13]. Values of the dissociation constants  $K_{dis}$  of complex MF with CDs evaluated by ATR-FTIR and UV-spectroscopy are summarized in Table 1.

The results of two approaches applied for  $K_{dis}$  measurements are in a good agreement, with ATR-FTIR method being superior in accuracy (Table 1), at the same time providing additional information on structural features involved in complex formation. The data obtained are in a good agreement with literature data. Typical values of  $K_{dis}$  for guest-host complexes of drugs with CDs are of the same magnitude [21–23].

Thus, the thermodynamic stability of guest-host complexes of fluoroquinolones (FQ) with  $\beta$ -cyclodextrins, as well as main binding sites and involvement of certain functional groups in complex formation were determined. To validate our conclusions based on ATR-FTIR data, 3D molecular modeling with energy optimization was carried out for FQ-CD complexes.

### Molecular modeling with energy optimization of MF and LF complexes with CDs

First of all, it should be noted that during all trajectories molecules in complexes remained bound to each other, which indicates complexes stability. The molecular modeling experiments show that in acidic media (where carboxylic group is protonated while the nitrogen in FQs heterocycles are positively charged) the complex formation of MF with all CDs studied here leads to penetration of MF aromatic core into the inner cavities of CD. This is

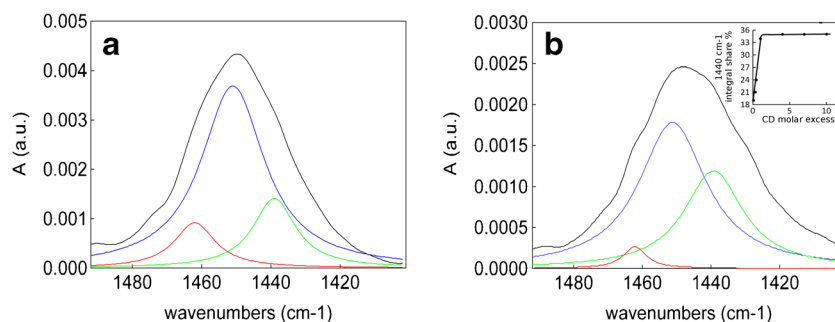


**Fig. 5** Deconvolution of the ATR-FTIR spectra region corresponding to adsorption of C-C band in benzene ring of MF (a) and MF-MCD 1:10 complex (b). MF concentration 1 mg/ml, pH 4, 22 °C. Insertion:

Dependence of the relative integral intensity of component at  $1440\text{ cm}^{-1}$  on the molar excess of MCD

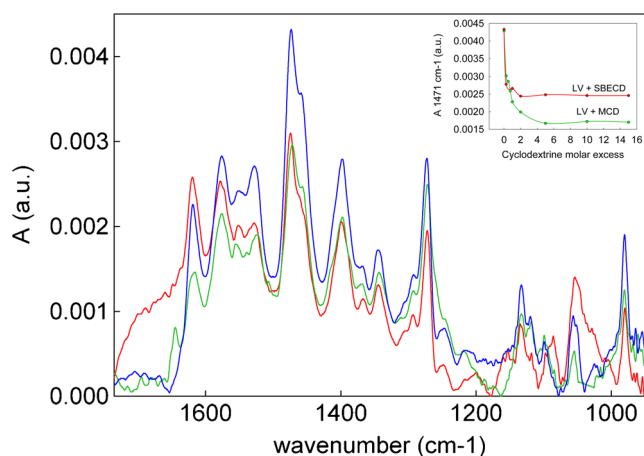
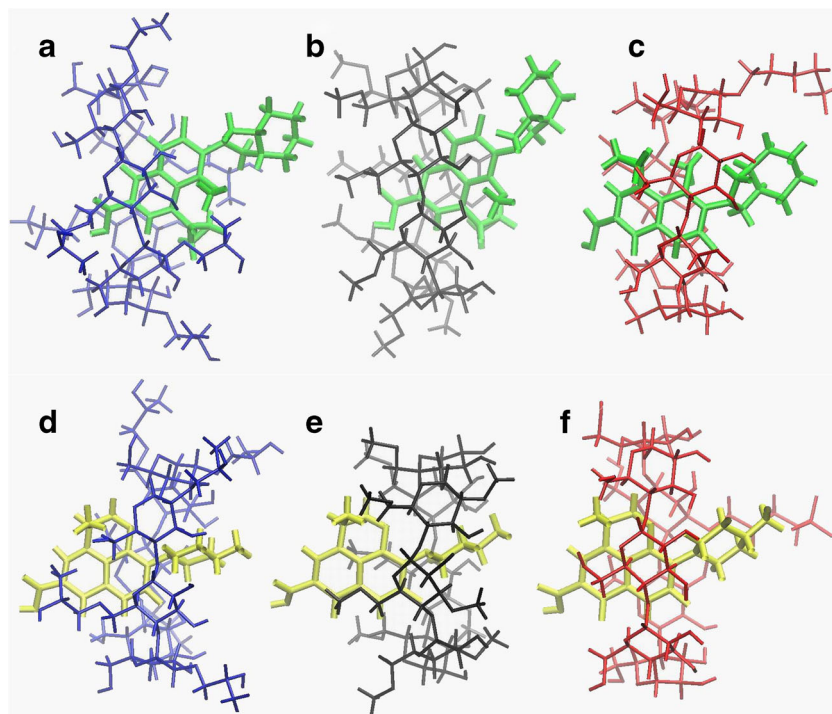


**Fig. 6** ATR-FTIR spectra of LF (blue line) and complex LF–MCD 1–1 (red line), LF–SBECD 1–1 (green line). LF concentration was 1 mg/mL, pH 4, 22 °C. Spectrum of corresponding CD has been subtracted as a blank. Insertion: Dependence of the C–C aryl band intensity at 1440  $\text{cm}^{-1}$  on CDs molar excess

thermodynamically favorable due to maximization of hydrophobic interactions area (Fig. 7a–c). In addition, the complexes are stabilized by hydrophobic interactions between cyclopropane ring of MF and substituents of the CDs: hydroxypropyl in HPCD, methyl group in MCD, or  $\text{CH}_2\text{OH}$  groups of glycoside residues in the case of SBECD. In the case of MCD, multiple hydrophobic interactions between aromatic core of MF and methyl groups of MCD stabilize the complex even further (Fig. 7b). Moreover, fluctuating hydrogen bonds are formed between carboxyl groups and CD-bound water molecules (most likely, connected with  $\text{CH}_2\text{OH}$  groups of CD).

**Fig. 7** The proposed structures of the complexes of MF with **a** HPCD, **b** MCD, and **c** SBECD and of the complexes of LF with **d** HPCD, **e** MCD, and **f** SBECD according to molecular modeling



The position of nitrogen-containing heterocyclic moiety of MF in the complexes depends on the substituent in CD. Figure 7a displays that in case of HPCD heterocycle is not involved in the complex formation; in the case of SBECD (Fig. 7c), a metastable fluctuating electrostatic bond between sulpho group and protonated nitrogen of MF heterocycle is formed, whereby the complex becomes more stable. For the complex with MCD multiple hydrophobic interactions with MF are observed. Complex with MCD has the most compact structure, which is the most thermodynamically favorable. These results are in agreement with the values of dissociation constants of the complexes obtained from ATR-FTIR spectra analysis (Table 1).

It is important to note that geometry of CDs is also changed upon the complex formation with MF. The flattening of CD torus perpendicularly to the plane of the aromatic core MF is observed. As the result, the diameter of the inner cavity in such deformed torus decreases by approximately 1 Å.

LF is prone to form complexes of another structure: the inclusion of the aromatic core of FQ into the inner cavity of the CDs is observed (Fig. 7d–e). The hydrophobic backbone of the molecule is strictly perpendicular to the plane of the CD torus. However, LF is located deeply in CD cavity in comparison with the complexes CD–MF. The position of LF relative to CD is the same regardless of the substituent in the CD. Additional stabilization of the complexes is realized by hydrophobic interactions between the methyl group in LF and the substituents in CD: methyl groups for MCD,  $\text{CH}_2\text{OH}$  groups for the HPCD and SBECD. Moreover, hydroxypropyl group in HPCD and a methyl in MCD are involved in hydrophobic

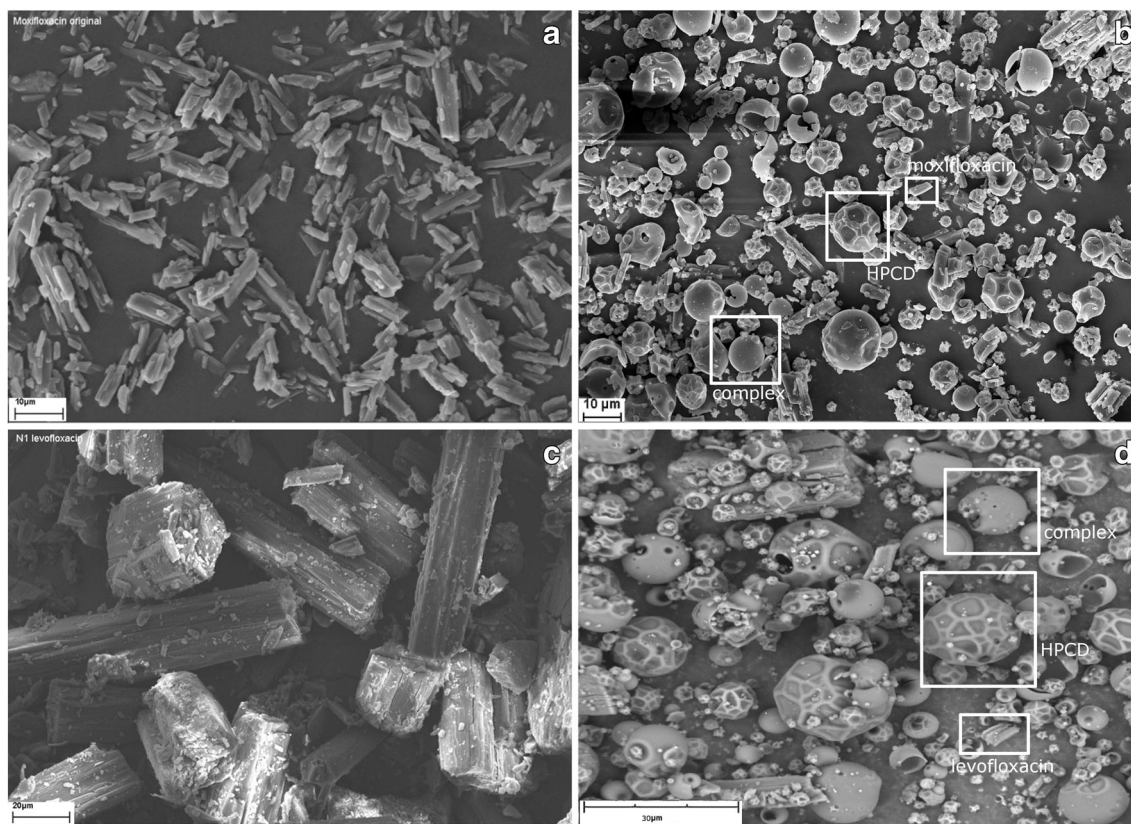


**Fig. 8** Morphology of MF and LF samples. **a** MF. **b** Complex MF–HPCD. **c** Levofloxacin. **d** Complex LF–HPCD studied by SEM

interactions with the aromatic structure of LF. In the case of MCD, these interactions are much more efficient, making complex LF–MCD more stable compared to LF–HPCD. This result is in agreement with dissociation constants of the complexes obtained by IR spectroscopy, which are differ by an order of magnitude ( $1.1 \times 10^{-4}$  M for LF–MCD versus  $1.1 \times 10^{-3}$  M for LF–HPCD). For SBECD, the formation of fluctuating electrostatic bond between  $\text{SO}_3$  group and protonated nitrogen in piperazol moiety of LF is observed. As for MF, LF carboxyl group is linked to the  $\text{CH}_2\text{OH}$  groups of CD through the formation of H bonds via water molecules. However, in contrast to the complexes of MF, protonated nitrogen in piperazol cycle in LF is also involved in the formation of H bonds with  $\text{CH}_2\text{OH}$  groups of CD regardless of the substituent in the CD. Apparently, this is due to the same position of LF molecule in all of the complexes studied. Values of the energy of complex formation are in good correlation with values of  $K_{\text{dis}}$  determined by ATR-FTIR (Table 1).

Comparing complexes with MF and LF, in the case of MF, due to its more pronounced hydrophobic properties, the most stable complexes are formed with CD carrying hydrophobic substituent, while in case of LF H bonds and electrostatic interactions make noticeable contribution in complex stabilization; thus, the most stable complex is LF–SBED.

The energy of complex formation might be used for interpretation of experimental data. It should be noted that all values of the energies of complex formation are of the order of  $(-16)$ – $(-35)$  kcal/mol. The negative values indicate that complex formation is more preferable for FQ than the free state in the aqueous phase. For MF, as an example, the energies of complex formation are  $-15.95$  and  $-19.59$  kcal/mol for MF–HPCD and MF–MCD. Indeed the experimental data confirms that the dissociation constant for MF complex with MCD is lower than with HPCD.

The lowest value of the energy of complex formation is related to the equilibrium complex between SBECD and MF:  $-32.08$  kcal/mol, due to the favorable electrostatic interactions between the sulfonic group of CD and the protonated nitrogen in MF. However, the strength of these interactions depends on favorable geometry of molecules, which fluctuate during dynamics simulation making highly variable.

Thus, data from molecular dynamics simulations proved a stable nature of studied complexes and reproduced their relational affinity and correlation with the experimental measured  $K_{\text{dis}}$ .

So, it should be noted that only in the case of MF the oligosaccharide torus undergoes flapping, due to stronger hydrophobic effects. In case of CD carrying polar side groups (HPCD), more complete inclusion of the aromatic

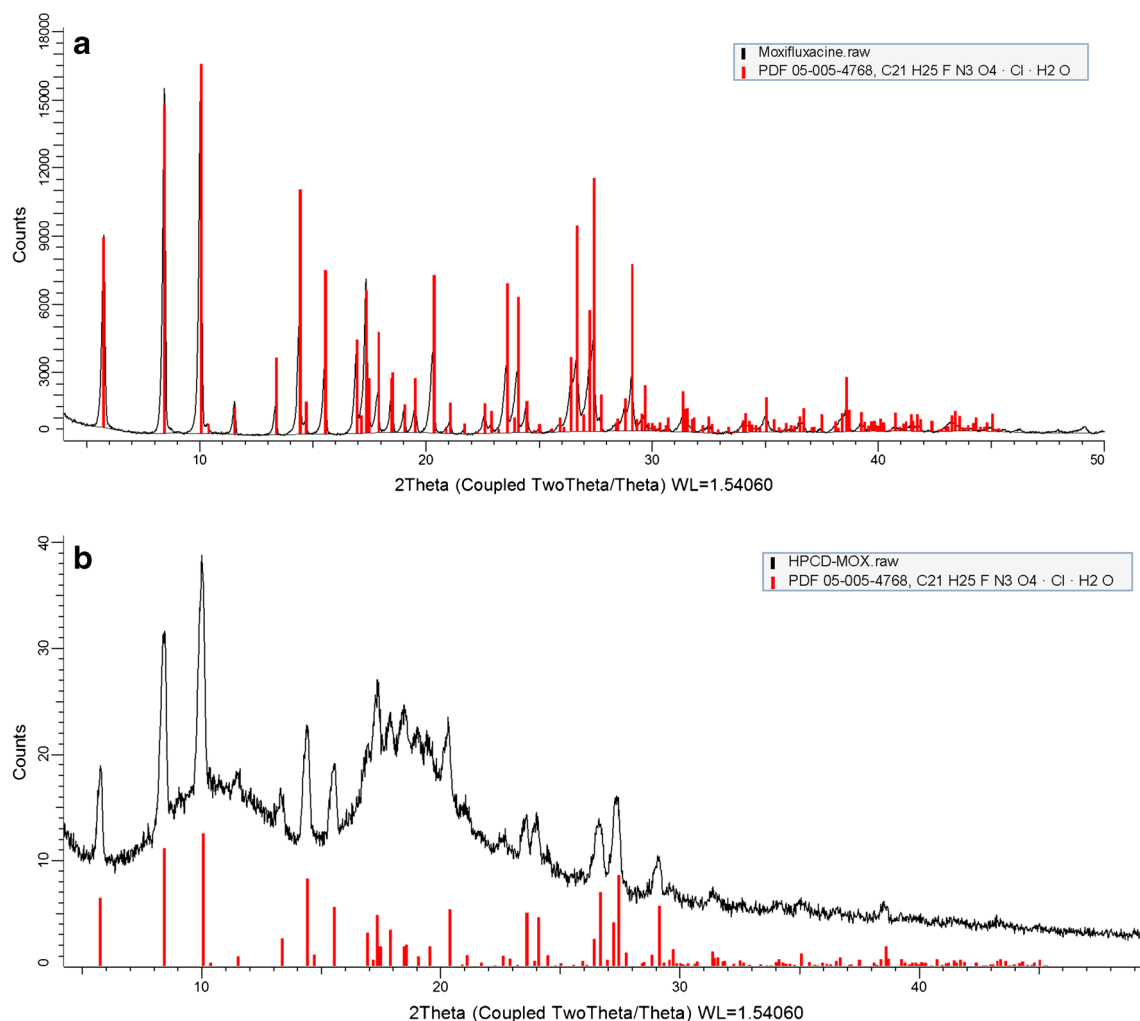


**Fig. 9** X-Ray diffractograms of **a** MF and **b** complex MF–HPCD

core is observed for LF; additional stabilization of the complex by interaction with hydroxypropyl radicals provides more efficient complex formation of HPCD with LF than that with MF. This is in agreement with dissociation constants obtained by spectroscopic methods ( $1.0 \times 10^{-3}$  M (for LF) versus  $3.3 \times 10^{-3}$  M (for MF)). In the case of MCD, methyl groups interact with aromatic structures of both FQ. However, MCD forms more compact and profitable complex with MF due to formation of multiple hydrophobic interactions. Thus, the complex MF–MCD is more stable ( $5.0 \times 10^{-5}$  M (for MF) versus  $1.0 \times 10^{-4}$  M (for LF)). In the complex with SBECD interaction with LF is more efficient, due to the participation of the nitrogen atom in piperazol group not only in the formation of electrostatic bonds but also in the formation of hydrogen bonds with  $\text{CH}_2\text{OH}$  groups CD through water molecules. Similar results have been obtained for ofloxacin–cyclodextrin system by other scientific groups, i.e., by Toth [24].

Therefore, the mechanism of complex formation suggested on the basis of ATR-FTIR data is confirmed by our molecular

modeling experiments as well as by calculations of the independent researchers.

### Scanning electron microscopy

Size and morphology of freeze-dried FQ–CD complexes have been studied by scanning electron microscopy (SEM). According to SEM, moxifloxacin particles are presented as prismatic prolonged crystals with average size of  $\sim 10$ – $20$   $\mu\text{m}$  (Fig. 8a); HPCD particles  $\sim 10$ – $20$   $\mu\text{m}$  possess spherical shape with porous surface according to previously obtained data [25] (Fig. 8b) and levofloxacin particles of  $\sim 40$ – $60$   $\mu\text{m}$  (Fig. 8c). The complex formation of MF with HPCD resulted to formation of new phase of spherical smooth particles of  $3$ – $4$   $\mu\text{m}$  in size (Fig. 8b). The particles of MF crystals and unbound CD are presented in the system as well. Similar phenomenon was observed comparing SEM images for LF and LF–HPCD (Fig. 8d). These pictures clearly elucidated the difference between LF and its inclusion complex (Fig. 8c, d), which supports the formation of inclusion complexes.

## X-ray analysis

Crystallinity of MF and its complexes with CD was studied on the example of complex MF–HPCD in comparison with MF by diffractometry. Figure 9a shows the results of X-ray measurements of MF and qualitative analysis in EVA program on the basis of PDF-4 Organic data. The XRD pattern of the sample corresponds to a crystalline moxifloxacin (PDF 05-005-4768). Figure 9b represents results for lyophilized complex MF–HPCD. The main components of this sample are the amorphous phase and the crystalline MF; the degree of crystallinity measured at the integral intensities of the “halo” and crystalline peaks is around 20%. Thus, the formation of complexes does not lead to changes in MF peaks, indicating that MF is not subjected to the transition to another polymorph. Hence, for MF complexes, there is a significant increase in the proportion of the amorphous phase up to 80%, which is formed by complex MF–HPCD. The data indicates a high efficiency of MF inclusion in the complex. It should be noted that increasing the proportion of the amorphous phase upon complex formation with the CD was also observed for other drug substances, particularly for the taxifolin [26].

Lower capacity for crystal formation may be a valuable pharmacokinetic feature for intravenous formulations of MF and LF, since they are known to form microcrystals in blood and kidney upon injection. One may anticipate that in complex with CD the spike of  $C_{\max}$  would be smoothed, thus avoiding crystallization.

## Conclusions

A new analytical tool enables direct spectroscopic measurements of non-covalent complex binding parameters and, combined with in silico 3D modeling, can provide insight in the structural features involved in binding and ways to improve it. Here, we have used FQ–CD as an example, showing the binding constant improvement by more than an order of magnitude, depending on side group substituents. The most efficient binding was observed for moxifloxacin and methyl–CD. 3D molecular modeling shows that in the complex with MCD the formation of multiple hydrophobic interactions between  $\text{CH}_3$  groups and MF hydrophobic sites is observed. Thus, complex with MCD has the most compact and the most thermodynamically favorable structure. For LF–SBECD, the binding constant is about 10-fold higher than that for LF–HPCD, indicating the importance of electrostatic interactions for stable complex formation. Indeed, the molecular modeling experiment yields that interaction of LF with SBECD is more efficient compared to LF–HPCD, due to the participation of the nitrogen atom in piperazol group in the formation of electrostatic bonds with sulphobutyl group. Thus, the proposed method based on ATR-FTIR spectroscopy can serve as a valuable

analytical tool for fundamental studies as well as for the development of controlled-release pharmaceutical formulations, such as involving FQs and CDs for anti-TB therapy. Obviously, the same approach can be applied for other non-covalent complexes as well, replacing inaccurate and time-consuming methods.

**Acknowledgments** This research is supported by RSF 15-13-00063. The authors thank Dr. Vinogradov A.A. for his comments on an earlier version of the manuscript and fruitful discussions and Dr. Putilin S.N. (Bruker AXS GmbH) for the help in X-ray experiments.

**Author contributions** The manuscript was written through contributions of all authors. All authors have given approval to the final version of the manuscript.

## Compliance with ethical standards

**Conflict of interest** The authors declare that they have no conflict of interest.

## References

1. Rubinstein E. History of quinolones and their side effects. *Chemotherapy*. 2001;47(suppl 3):3–8.
2. Ahmad Z, Pandey R, Sharma S, Khuller GK. Novel chemotherapy for tuberculosis: chemotherapeutic potential of econazole- and moxifloxacin-loaded PLG nanoparticles. *Int J Antimicrob Agents*. 2008;31(2):142–6.
3. Zhang J, Ma PX. Cyclodextrin-based supramolecular systems for drug delivery: recent progress and future perspective. *Adv Drug Deliv Rev*. 2013;65(9):1215–33.
4. Misiuk W, Jozefowicz M. Study on a host–guest interaction of hydroxypropyl-B-cyclodextrin with ofloxacin. *J Mol Liq*. 2015;202:101–6.
5. Drevenšek P, Košmrlj J, Giester G, Skauge T, Slette E, Sepčić K, et al. X-ray crystallographic, NMR and antimicrobial activity studies of magnesium complexes of fluoroquinolones—racemic ofloxacin and its S-form. *Levofloxacin J Inorg Biochem*. 2006;100(11):1755–63.
6. Elbashir AA, Dsugi NFA, Aboul-Enein HY. Supramolecular study on the interaction between ofloxacin and methyl B-cyclodextrin by fluorescence spectroscopy and its analytical application. *J Fluoresc*. 2014;24:355–61.
7. Mamian-Lopez MB, Poppi RJ. Quantification of moxifloxacin in urine using surface-enhanced Raman spectroscopy (SERS) and multivariate curve resolution on a nanostructured gold surface. *Anal Bioanal Chem*. 2013;405(24):7671–7.
8. Sousa J, Alves G, Fortuna A, Falcão A. Analytical methods for determination of new fluoroquinolones in biological matrices and pharmaceutical formulations by liquid chromatography: a review. *Anal Bioanal Chem*. 2012;403(1):93–129.
9. Deygen IM, Kudryashova EV. New versatile approach for analysis of PEG content in conjugates and complexes with biomacromolecules based on FTIR spectroscopy. *Colloids Surf B Biointerfaces*. 2016;141:36–43.
10. Deygen IM, Egorov AM, Kudryashova EV. Structure and stability of Fluoroquinolone-(2-hydroxypropyl)-B-cyclodextrin complexes as perspective antituberculosis drugs. *Mosc Univ Chem Bull*. 2016;71(1):1–6.

11. Kudryashova EV, Deygen IM, Sukhoverkov KV, Filatova LY, Klyachko NL, Vorobei AM, et al. Micronization of levofloxacin by supercritical antisolvent precipitation. *Russ J Phys Chem B*. 2016;10(4):52–66.
12. Kudryashova EV, Sukhoverkov KV, Deygen IM, Vorobey AM, Pokrovskiy OI, Parenago OO, et al. Influence of parameters of moxifloxacin micronization by anti-solvent precipitation on its physic-chemical properties. *Supercrit Fluids Theory Pract*. 2016;11(3):71–85.
13. Hendy GM, Breslin CB. A spectrophotometric and NMR study on the formation of an inclusion complex between dopamine and a sulphonated cyclodextrin host. *J Electroanal Chem*. 2011;661(1): 179–85.
14. Gunasekaran S, Rajalakshmi K, Kumaresan S. Vibrational analysis, electronic structure and nonlinear optical properties of levofloxacin by density functional theory. *Spectrochim Acta A Mol Biomol Spectrosc*. 2013;112:351–63.
15. Goyne KW, Chorover J, Kubicki JD, Zimmerman AR, Brantley SL. Sorption of the antibiotic ofloxacin to mesoporous and nonporous alumina and silica. *J Colloid Interface Sci*. 2005;283(1):160–70.
16. Pandey S, Pandey P, Tiwari G, Tiwari R, Rai AK. FTIR spectroscopy: a tool for quantitative analysis of ciprofloxacin in tablets. *Indian J Pharm Sci*. 2009;71(4):359–70.
17. Sahoo S, Chakraborti CK, Mishra SC, Naik S, Nanda UN. FTIR and Raman spectroscopy as a tool for analyzing sustained release hydrogel of ciprofloxacin/carbopol polymer. *Int J Pharm Sci Res*. 2011;2(2):268–77.
18. Tomren MA, Måsson M, Loftsson T, Tønnesen HH. Studies on curcumin and curcuminoids. XXXI. Symmetric and asymmetric curcuminoids: stability, activity and complexation with cyclodextrin. *Int J Pharm*. 2007;338(1–2):27–34.
19. Saenger W. Cyclodextrin inclusion compounds in research and industry. *Angew Chem Int Ed Engl*. 1980;19(5):344–62.
20. Stella VJ, He Q. Cyclodextrins. *Toxicol Pathol*. 2008;36(1):30–42.
21. Jelić R, Tomović M, Stojanović S, Joksović L, Jakovljević I, Djurdjević P. Study of inclusion complex of  $\beta$ -cyclodextrin and levofloxacin and its effect on the solution equilibria between gadolinium(III) ion and levofloxacin. *Monatshefte für Chemie - Chem Mon*. 2015;146(10):1621–30.
22. Dsugi NFA, Elbashir AA. Supramolecular interaction of moxifloxacin and  $\beta$ -cyclodextrin spectroscopic characterization and analytical application. *Spectrochim Acta A Mol Biomol Spectrosc*. 2016;137:804–9.
23. Jambhekar SS, Breen P. Cyclodextrins in pharmaceutical formulations II: solubilization, binding constant, and complexation efficiency. *Drug Discov Today*. 2016;21(2):363–8.
24. Tóth G, Mohácsi R, Rácz A, Rusu A, Horváth P, Szente L, et al. Equilibrium and structural characterization of ofloxacin–cyclodextrin complexation. *J Incl Phenom Macrocycl Chem*. 2013;77(1): 291–300.
25. Bandi N, Wei W, Roberts CB, Kotra LP, Kompella UB. Preparation of budesonide– and indomethacin–hydroxypropyl- $\beta$ -cyclodextrin (HPBCD) complexes using a single-step, organic-solvent-free supercritical fluid process. *Eur J Pharm Sci*. 2004;23:159–68.
26. Zu S, Yang L, Huang J, Ma C, Wang W, Zhao C, et al. Micronization of taxifolin by supercritical antisolvent process and evaluation of radical scavenging activity. *Int J Mol Sci*. 2012;13(7): 8869–81.